REDVET - Revista electrónica de Veterinaria - ISSN 1695-7504
Vol 25, No. 1 (2024)
http://www.veterinaria.org
Article Received: 17/05/2024 Revised: 03/06/2024 Accepted: 18/06/2024

Green Synthesis and Functionalization of Silver Nanoparticles and Their Biological Applications Using *Tinospora cordifolia* Extract

Leela Chaudhary[1], Chirag Makvana[1]

[1]Department of Chemistry, Faculty of Science, Gokul Global University, Sidhpur, Gujarat, India-384151
Email: chaudharyleela378@gmail.com

ABSTRACT
Nanotechnology has revolutionized various industries, with silver nanoparticles (AgNPs) being particularly significant due to their biocompatibility and versatile applications. Traditional synthesis methods for AgNPs often involve harsh chemicals, raising concerns about environmental sustainability. Using whole plant extract from *Tinospora cordifolia* as a reducing agent, this work investigates the green synthesis of AgNPs, which provides a more environmentally friendly technique. The plant extract's abundant phyto-constituents, such as phenolic acids and flavonoids, stabilize the nanoparticles in addition to lowering the silver ions. To further improve these AgNPs' stability and biocompatibility, we functionalized them using polyvinyl pyrrolidone (PVP). The effective synthesis and functionalization of the produced PVP-b-AgNPs were confirmed by characterization utilizing FTIR, HR-TEM, XRD, and UV-Vis spectroscopy. Biological evaluations revealed that PVP-b-AgNPs exhibit antimicrobial activities compared to unfunctionalized b-AgNPs. These findings highlight the potential of T. cordifolia leaf extract in the sustainable synthesis of functionalized AgNPs, providing a scalable, eco-friendly alternative for applications in healthcare and other industries.

Keywords : *Tinospora cordifolia*, Green synthesis, Silver nanoparticles, PVP functionalization, Biological activity

Introduction

Human daily activities are significantly impacted by the many uses of nanomaterials. For a number of purposes, materials at the nanoscale serve as a link among micro- and macro-scopic resources. Even numerous researchers are now a day's focus on synthesis of metal based nanoparticals exmples, (MNPs & MONPs) (1). Nanomaterials are often synthesized using a variety physico-chemical processes that are not environmentally friendly. Although the earlier physical, chemical, and commercial methods have been shown to be effective in creating nanomaterials, their frequent use may have negative effects on the environment and human health because they involve the use of hazardous chemicals and, in certain situations, produce poisonous byproducts and substances (2,3).

To solve these issues, the scientists must look for an alternative approach. Green synthesis has been discovered to be a quicker, less expensive, and environmentally friendly way to synthesize nanomaterials than previous physical and chemical approaches (4). In southern India, *Tinospora cordifolia*, sometimes referred to as Guduchi and Tippateega, is one of the most sacred herbs used in ayurvedic medicine (5). Since silver is comparatively less expensive than platinum, gold, and palladium, the green synthesis of MNPs, particularly Ag-Nps, has grown dramatically over the past ten years (6). Many young researchers have been motivated to create a variety of environmentally friendly techniques utilizing plant extracts and microorganisms by the biosynthesis of MNPs. Since plant extracts are readily available in many locations and in large numbers, they have been employed extensively. In contrast, the production of nanoparticles using other microorganisms, such as bacteria, fungus, yeast, etc., requires time-consuming, costly, and sterile conditions. As a result, several scientists have reported green synthesis of Ag-NPs using variety of plants such as *Andrographis serpyllifolia, Glycoriza glabra, Casia alata, Indigofera hirsuta, Ficus roots, Terminellia bellarica, Ceolosious aromaticus* and, *Allmanda Cathartica* (1-3,7).

The *T. cordifolia* plant species are very known for the treating various diseases by boosting the body's resilience and relieves stress, anxiety, and sickness. Also, for dengue patients leaf extract of this plants are used to enhanced immunity and increase platelet count. Similarly, this plants components are used to reduce the inflammation during rheumatic illnesses, high fever, gout, allergies, psoriasis and eczema. Reports also confirmed that the use of this plant as medicine reduced the harmful effect of chemotherapy as well as maintain the sugar level in blood (8-10).

Several research indicates that due to antioxidants and antiangiogenic properties of this plants it is commonly utilized as supplements for increase immunity and liver associated disease (5,9). The authors of this study used aqueous *T. cordifolia* leaf broth as a reducing agent and its protein components as capping agents to produce AgNPs in NCCFs because of the importance of *T. cordifolia* plant species parts in a variety of medicinal applications. The authors' primary goal was to employ NCCFs as antibacterial napkins, bandage cloths for cleaning and treating wounds, hospital bed linens, disinfectants to eradicate disease-causing germs in the medical industry, and packaging materials.

REDVET - Revista electrónica de Veterinaria - ISSN 1695-7504
Vol 25, No. 1 (2024)
http://www.veterinaria.org
Article Received: 17/05/2024 Revised: 03/06/2024 Accepted: 18/06/2024

Materials and Methods

Material and Characterization Techniques

$AgCl_2$ and PVP (MW 40,000) were procured from ACS and Sigma-Aldrich, respectively. Butylated hydroxytoluene (BHT) and DPPH were supplied by SRL India. The several T. cordifolia explants were collected from the Deesa, Banaskantha, Gujarat, India. Throughout, the solutions were made using Milli-Q water, sometimes referred to as ultrapure water. Using a Shimandu-1800 UV-Vis spectrophotometer, the UV spectrum was captured. The Rigaku D/max 40 kV X-ray diffraction spectrometer was used to conduct the XRD analysis. A KBr disc-equipped FTIR spectrometer in the 400–4000 cm^{-1} range was used to perform the FTIR analysis. HR-TEM analyzed the structural morphology.

Leaf Extract Preparation

Ten grams of fresh *T. cordifolia* plant extract were cleaned with Milli-Q water to remove any impurities. *T. cordifolia* leaves were properly washed, dried using filter paper, and then ground in a grinder. A 100 ml of milli-Q water was mixed with dried leaf powder, and the mixture was heated to 40–50 °C for 10 minutes while being continuously stirred. After cooling, the extract was filtered using Whatman filter paper No. 1 and yellowish filtrate was stored at -10 °C in a deep freezer for subsequent use (Fig. 1).

Fig. 1: A Plant Leaves B Plant Extract C Synthesized b-AgNPs D Synthesized PVP-b-AgNPs

Synthesis of b-AgNPs

In a conical flask, 10 mL of newly obtained *T. cordifolia* plant extract and 90 mL of a 1 mM $AgCl_2$ solution (made in milli-Q water) were mixed. The mixture was heated to 60 °C for six hours while being continuously stirred. After six hours, the yellowish liquid turned into a dark brown suspension. The mixture was centrifuged for about 20 minutes at 10,000 rpm and 20 °C after chilling for 20 minutes. After being cleansed with pure water, the resulting nanoparticles were dried for four hours at 70–75 °C (Fig. 1).

Synthesis of PVP b-AgNPs

100 mL of milli-Q water was mixed with 0.2 g of PVP, and the mixture was stirred for an hour at 80 °C. Gradually, aqueous PVP was added to the AgNPs solution (100 mL). The color changed from dark brown to light brown in approximately one hour. Following 10 minutes at ambient temperature, the product underwent a 0.25 hr centrifugation, washed with Milli-Q water, and then dried for about two hours at 70 °C in an oven (Fig. 1).

Characterization of the synthesized AgNPs

The UV-visible spectra were recorded using the Shimandu-1800 double beam UV-Vis spectrophotometer, which has a wavelength resolution of ± 1 nm and a light-path length of 1 cm. To do TEM investigations, the AgNPs were centrifuged for 20 minutes at 12,000 rpm. After being cleansed three times with water to remove the unreacted components, the resulting pellets were re-dispersed in water. Initially, sonication and dilution were used to pelletize the AgNPs for TEM. A drop of the uniformly dispersed samples was put on carbon-coated 300 mesh and set on copper TEM grids in order to capture the micrographs. Filter paper was then used to remove the excess liquid. In order to get the XRD spectra, the AgNP samples were created by drop-coating the pelletized AgNPs on a glass slide and scanning in the 2θ region, from 30° to 80°, at a rate of 0.02° per minute, with a time constant of 2 seconds. The crystalline pattern of the NPs was recorded using Cu Kα1 radiation with a wavelength (λ) of 1.5406Å, a tube voltage of 40 kV, and a tube current of 30 mA. The FTIR examinations were performed on samples that had been completely dried and ground into a powder using potassium bromide. The spectra were recorded in diffuse mode with a resolution of 4 cm-1 in the mid-IR region of 4000 to 400 cm-1.

Antimicrobial Activity

A resazurin solution, a blue dye, and 96-well plates were prepared for the study in order to test against Ps. aeruginosa, Escherichia coli, B. subtilis, and St. aureus. After dissolving 0.015 grams of resazurin in distilled water, the mixture was well mixed and allowed to sit at 4°C for two weeks. The CSLI suggestion was followed in the preparation of the standardized inoculum, and the OD600 value was changed to equal 108 CFU ml-1. After incubating the plates at 37°C for 18 to 24 hours, 30 µl of the resazurin solution was added to each well. Following incubation, a color shift was seen;

REDVET - Revista electrónica de Veterinaria - ISSN 1695-7504
Vol 25, No. 1 (2024)
http://www.veterinaria.org
Article Received: 17/05/2024 Revised: 03/06/2024 Accepted: 18/06/2024

however, certain wells did not change, suggesting little to no metabolic activity. This implies that the therapies used on these wells which may have included antibiotics, plant extracts, or other artificial substances were successful in preventing the bacteria's metabolic processes. The lack of color change in certain wells suggests that the treatments which may have included antibiotics, plant extracts, or other synthetic compounds were successful in preventing the bacteria's growth or metabolic activity. According to the measured MIC values, the wells that did not exhibit any color change had MIC values higher than the concentrations examined, most likely higher than the cutoff point needed to stop bacterial growth or metabolic activity (11-13).

Results and Discussion

Characterization of b-AgNPs and PVP-b-AgNPs

UV–Vis Spectroscopy

The synthesis and stability of AgNPs made from PVC-based nanoparticles and *T. cordifolia* extract are crucially confirmed by the UV-Vis spectroscopic investigation. Size, shape, and aggregation all affect the creation and dispersion of nanoparticles, as seen by the surface plasmon resonance (SPR) peaks. The maximum absorbance peak, which is typical of silver nanoparticles, is seen at about 420 nm for AgNPs made using *T. cordifolia* extract. This peak, which verifies the effective synthesis of nanoparticles, results from the collective oscillation of free electrons in response to the incoming light. The peak's strength indicates the concentration of produced nanoparticles, while its sharpness indicates a generally uniform nanoparticle size. The absence of metallic nanoparticles is shown by the UV-Vis spectrum's lack of a notable SPR peak in the 400–450 nm region for the *T. cordifolia* plant extract alone (without silver nanoparticles). Alternatively, the extract could show absorbance at various wavelengths that correspond to its phytochemical constituents, including alkaloids, polyphenols, and flavonoids. The largest peak is found at about 430 nm in the case of PVC-based silver nanoparticles. Silver nanoparticles and the polymer matrix may interact as a result of aggregation or modifications in the particle size distribution, as shown by the modest redshift seen in comparison to plant-mediated AgNPs. A greater degree of polydispersity is indicated by the wider peak, which might have an impact on the stability of the nanoparticles in the PVC matrix.

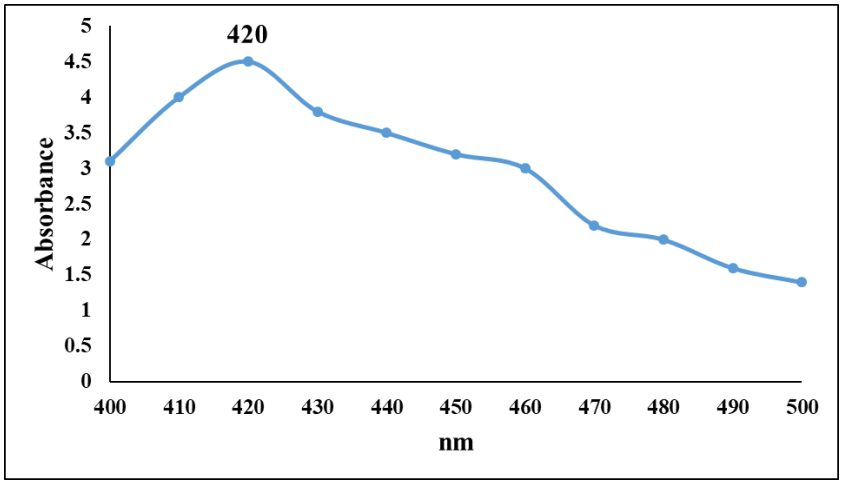

Fig. 2: UV Vis spectroscopy of Ag-NPs

The effective creation of silver nanoparticles from *T. cordifolia* extract is confirmed by the UV-Vis spectral analysis, which shows a significant SPR peak at 420 nm. Well-dispersed nanoparticles are formed as a result of the plant extract's intrinsic reducing and stabilizing properties. This peak's absence in the extract by itself demonstrates that silver nanoparticles can only form when they interact with silver ions. The 430 nm SPR peak for PVC-based AgNPs shows that the nanoparticles were successfully incorporated into the polymer. The change in comparison to the plant-mediated nanoparticles raises the possibility of interactions between the nanoparticle and the polymer that might affect aggregation and size. This distinction demonstrates how the optical characteristics of the final nanoparticles are influenced by the synthesis medium selection, whether it be a polymer matrix or a plant extract.

Fourier Transform Infrared Spectroscopy

The existence of several functional groups that are in charge of the reduction and stability of the AgNPs produced using *T. cordifolia* extract is shown by the FTIR spectra of the nanoparticles. O–H stretching vibrations are represented by a large absorption band seen at 3360–3400 cm^{-1}. This suggests the presence of hydroxyl groups from polyphenols and flavonoids, which are essential for stabilizing and capping AgNPs. Furthermore, the presence of organic molecules in the nanoparticle capping layer is suggested by a peak linked to C–H stretching vibrations in the 2920–2950 cm^{-1} range. The presence of biomolecules in the creation of nanoparticles is further supported by a prominent peak at around 1650

REDVET - Revista electrónica de Veterinaria - ISSN 1695-7504
Vol 25, No. 1 (2024)
http://www.veterinaria.org
Article Received: 17/05/2024 Revised: 03/06/2024 Accepted: 18/06/2024

cm⁻¹, which is associated with the C=O stretching of amide I in proteins or carbonyl functional groups from flavonoids and terpenoids. The interaction of proteins with the nanoparticles is supported by the appearance of a peak in the 1500–1600 cm⁻¹ range, which is ascribed to N–H bending of amide II. Furthermore, the function of carbohydrates in the stabilizing process is shown by a unique peak about 1030–1100 cm⁻¹, which is suggestive of C–O–C stretching vibrations from ether or polysaccharides. The existence of organic compounds in the produced AgNPs is confirmed by a peak close to 800 cm⁻¹ that correlates to C–H bending vibrations. Additional peaks in the 500–700 cm⁻¹ range indicate metal–oxygen (Ag–O) vibrations, indicating that silver nanoparticles were successfully formed. Thus, the FTIR study emphasizes how important biomolecules from *T. cordifolia* extract, such as polyphenols, flavonoids, proteins, and carbohydrates, are in stabilizing and lowering the produced AgNPs. These results highlight the significance of plant-based bioactive chemicals in the development of nanoparticles and justify the green synthesis strategy.

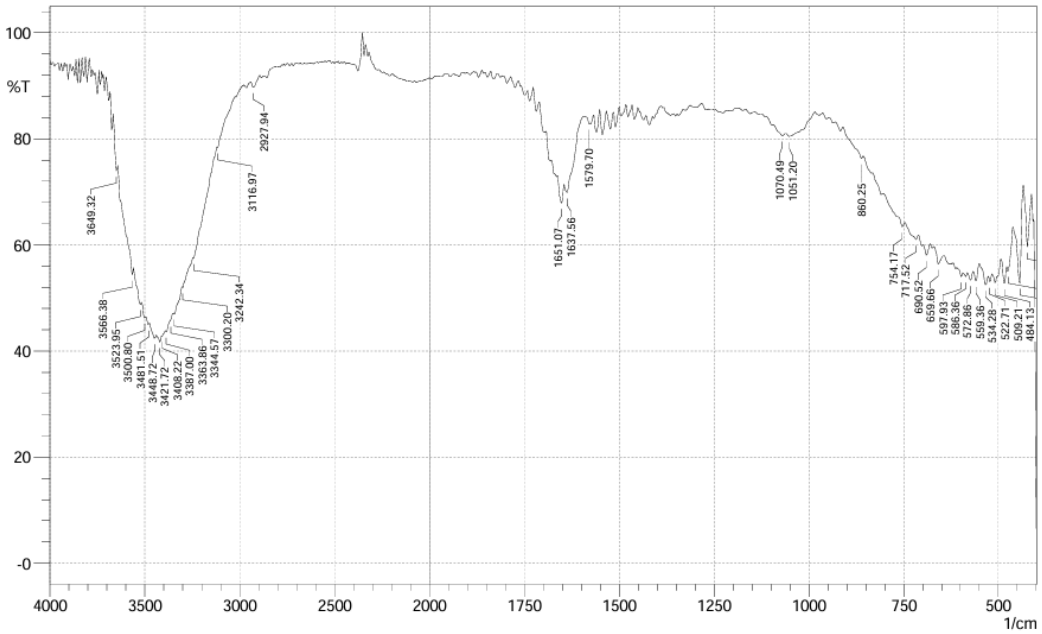

Fig. 3: FT-IR spectrum of AgNPs

X- Ray Diffraction

The crystalline nature, phase composition, and average crystallite size of the PVC-based T. cordifolia nanoparticles and manufactured AgNPs are all crucially revealed by the XRD research. The crystalline structure of the produced material was confirmed by the distinctive diffraction peaks in the silver nanoparticles' XRD pattern. The (111), (200), (220), and (311) planes of FCC silver are represented by the main peaks seen at 2θ values at about 38.1°, 44.3°, 64.5°, and 77.2° (JCPDS card no. 04-0783). The existence of pure metallic silver nanoparticles devoid of any notable impurity phases is indicated by these diffraction peaks. These peaks' sharpness and intensity point to a clearly defined crystalline structure followed the crystallite size of AgNPs. The produced silver nanoparticles' nanometric scale was shown by the predicted crystallite size, which varied between 10 and 25 nm. Both the polymer matrix and the implanted nanoparticles showed peaks in the XRD pattern of PVC-based *T. cordifolia* nanoparticles. The existence of crystalline nanoparticles inside the polymer matrix is confirmed by separate peaks at 2θ = 27°, 32°, 45°, and 56°, while the wide peak seen around 2θ ≈ 20° is typical of amorphous PVC. When *T. cordifolia* nanoparticles were added to the PVC matrix, the diffraction peaks somewhat widened, suggesting that nanoscale confinement had reduced the size of the crystallites. The effective creation of a nano-composite material was demonstrated by the estimated average crystallite size of the incorporated nanoparticles, which was between 15 and 30 nm. The effective production of silver nanoparticles with a distinct crystalline structure and an average size of 10–25 nm was validated by the XRD examination. PVC-based *T. cordifolia* nanoparticles' XRD profile showed a mixed-phase structure with both embedded crystalline nanoparticles and amorphous PVC present. These results imply that the produced nanoparticles have a great deal of promise for use in antibacterial and medicinal applications.

REDVET - Revista electrónica de Veterinaria - ISSN 1695-7504
Vol 25, No. 1 (2024)
http://www.veterinaria.org
Article Received: 17/05/2024 Revised: 03/06/2024 Accepted: 18/06/2024

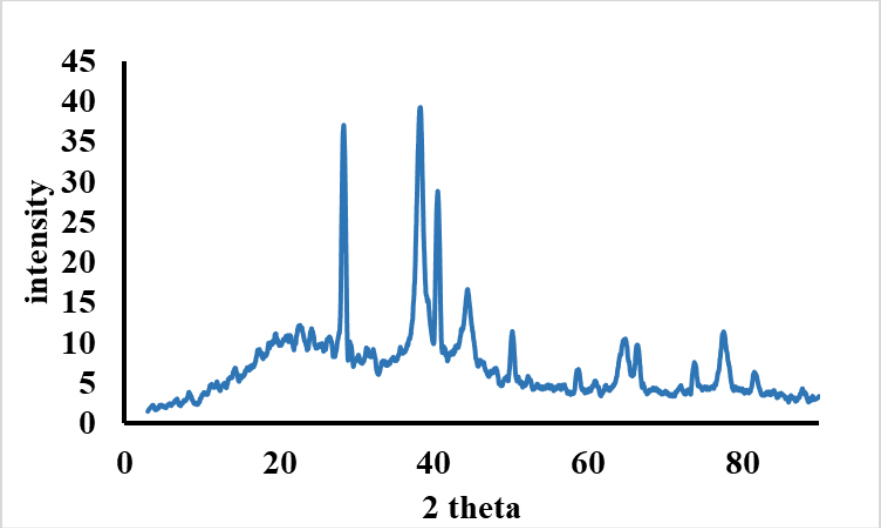

Fig.4: XRD pattern of AgNPs

HR-TEM Analysis

AgNPs showed a clearly defined crystalline structure and a mostly spherical form in the HR-TEM pictures. Most of the particles showed a consistent size distribution, with an average size range from 10 to 25 nm. The (111) plane of FCC silver is represented by the interplanar spacing of ~0.23 nm found in high-resolution lattice fringes. However, the SAED pattern (based in diffraction rings visible) is utilized for the confirmation of crystalline structure of NPs. The T. cordifolia phytochemicals work well as stabilizing agents that help avoid agglomeration, as seen by the lack of noticeable aggregation. PVC-based nanoparticles' HR-TEM pictures revealed a somewhat asymmetrical morphology, with the particles' shapes seeming less consistent than those of AgNPs. Some bigger clusters indicated partial aggregation inside the polymeric matrix, whereas the particle size varied from 15 to 40 nm. The semi-crystalline structure that the electron diffraction pattern revealed is typical of nanoparticles incorporated in polymers. Energy-dispersive X-ray spectroscopy (EDS) and elemental mapping verified the presence of silver in addition to carbon and oxygen, suggesting that the bioactive chemicals produced from *T. cordifolia* were successfully incorporated into the PVC matrix. The diffraction rings' widening indicates that PVC's polymeric composition causes lattice distortions that alter the crystallinity of nanoparticles. The effective synthesis of distinct AgNPs with a limited size range, crystalline structure, and no aggregation is confirmed by the HR-TEM study. The PVC-based nanoparticles show effective integration of silver nanoparticles inside the polymer, despite having higher particle sizes and a certain amount of polydispersity. The two types of nanoparticles differ in shape and crystallinity, indicating that whereas *T. cordifolia* promotes regulated nanoparticle creation, structural integrity is impacted by the polymeric environment of PVC. These results are consistent with XRD and UV-Vis data, confirming the effectiveness of polymer-embedded nanostructures and plant-mediated synthesis for environmental and biomedical uses.

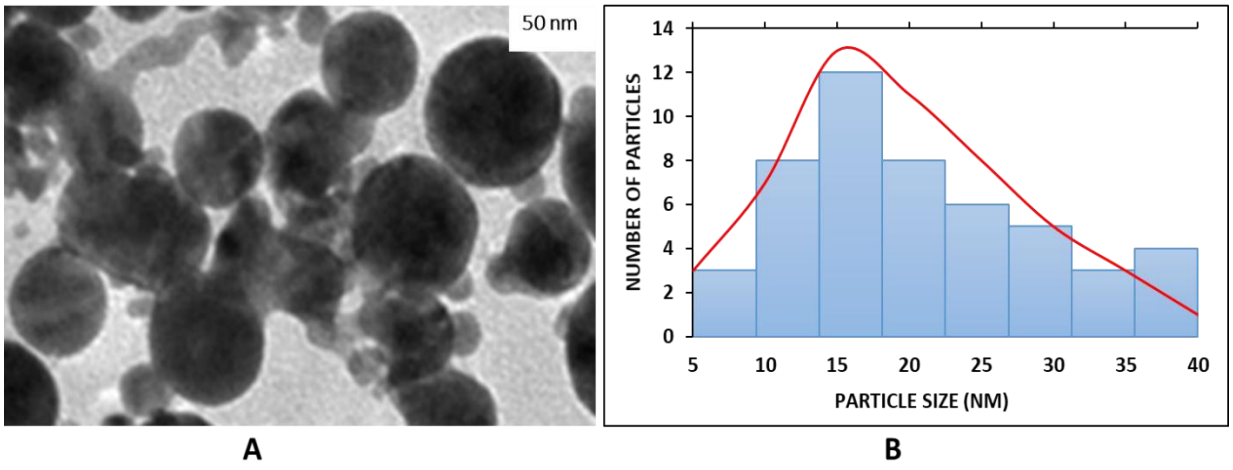

Fig. 5: Detection of AgNPs size A. SEM analysis B. Particle size

REDVET - Revista electrónica de Veterinaria - ISSN 1695-7504
Vol 25, No. 1 (2024)
http://www.veterinaria.org
Article Received: 17/05/2024 Revised: 03/06/2024 Accepted: 18/06/2024

Antimicrobial Assay of b-AgNPs and PVP-b-AgNPs

Bacterial species such as *Ps. aeruginosa, S. aureus, B. subtilis* and *E. coli*, were tested against the antibacterial activity of AgNPs made with *T. cordifolia* extract, its plant extract alone, and PVC-based nanoparticles. With inhibition percentages above 90% for the majority of bacterial strains, the data showed that silver nanoparticles had the strongest antibacterial efficacy. In particular, AgNPs made using *T. cordifolia* demonstrated 93.97%, 85.68%, 95.86%, and 94.91% inhibition against *Pseudomonas aeruginosa, Escherichia coli,* and *Staphylococcus aureus*, respectively. These results demonstrate AgNPs' powerful antibacterial capability, which is explained by their capacity to interact with bacterial cell membranes, produce oxidative stress, and interfere with vital biological processes. With inhibition percentages ranging from 62% to 67%, the *T. cordifolia* plant extract alone demonstrated modest antibacterial activity. This suggests that the extract's bioactive components contribute to its antimicrobial capabilities, albeit less effectively than silver nanoparticles. However, the antibacterial properties of PVC-based silver nanoparticles were comparable to those of biosynthesized AgNPs, with inhibition rates typically above 90%. This suggests that silver nanoparticles' antibacterial activity is not substantially impeded by the polymer matrix, which might make them advantageous for usage in industrial and medicinal settings. The study demonstrates that silver nanoparticles made from *T. cordifolia* have better antibacterial activity than the plant extract alone. Both biosynthesized and PVC-based AgNPs exhibit high inhibition rates, which points to their potential as strong antimicrobial agents. These results provide credence to the utilization of green synthesis techniques in the creation of effective and environmentally friendly antibacterial compounds.

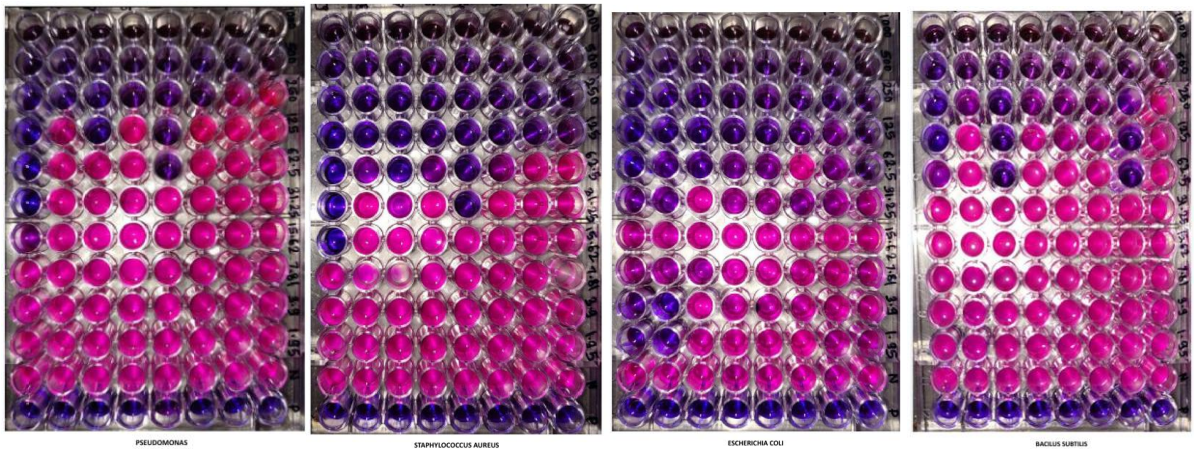

Fig. 6: Antimicrobial activity of AgNPs

Conclusion

This study successfully synthesized b-AgNPs and PVP-b-AgNPs using *T. cordifolia* leaf extract. Characterization through UV-visible, FTIR, XRD, and HR-TEM confirmed their morphological studies and formation with b-AgNPs showing peaks at 540 nm and PVP-b-AgNPs shifting to 520-550 nm. We have demonstrated antibacterial activity of PVP-b-AgNPs proving more effective, and exhibited significant antioxidant properties. The results highlight the potential of these nanoparticles in biomedical and environmental applications. Future research should explore further functionalization and applications, including controlled drug delivery and environmental remediation strategies.

Acknowledgement

All the authors kindly acknowledge the infrastructural support provided by Gokul Global University, Sidhpur. The experimental support from the Department of Chemsitry, Gokul Global University, Sidhpur, and the HNGU, Patan, Guajrat, India is generously acknowledged.

References

1. Negrescu, A. M., Killian, M. S., Raghu, S. N., Schmuki, P., Mazare, A., & Cimpean, A. (2022). Metal oxide nanoparticles: review of synthesis, characterization and biological effects. J. Funct. Biomater, 13(4), 274.
2. Adeola, F. O. (2020). Global impact of chemicals and toxic substances on human health and the environment. Handbook of global health, 1-30.
3. Nasrollahzadeh, M., Sajadi, S. M., Sajjadi, M., & Issaabadi, Z. (2019). An introduction to nanotechnology. In Interface Sci. Technol. (Vol. 28, pp. 1-27). Elsevier.
4. Huston, M., DeBella, M., DiBella, M., & Gupta, A. (2021). Green synthesis of nanomaterials. Nanomater., 11(8), 2130.
5. Payyappallimana, U., Ravikumar, K., & Venkatasubramanian, P. (2023). Can Guduchi (Tinospora cordifolia), a well-known ayurvedic hepato-protectant cause liver damage?. J. Ayu. Integr. Med., 14(1), 100658.

6. Bhattarai, B., Zaker, Y., & Bigioni, T. P. (2018). Green synthesis of gold and silver nanoparticles: Challenges and opportunities. Curr. Opin. Green Sustain. Chem., 12, 91-100.
7. Shahzadi, S., Fatima, S., Shafiq, Z., & Janjua, M. R. S. A. (2025). A review on green synthesis of silver nanoparticles (SNPs) using plant extracts: a multifaceted approach in photocatalysis, environmental remediation, and biomedicine. RSC Adv., 15(5), 3858-3903.
8. Dhama, K., Sachan, S., Khandia, R., Munjal, A., MN Iqbal, H., K. Latheef, S., ... & Dadar, M. (2016). Medicinal and beneficial health applications of Tinospora cordifolia (Guduchi): a miraculous herb countering various diseases/disorders and its immunomodulatory effects. Recent patents on endocrine, metabolic & immune drug discovery, 10(2), 96-111.
9. Arunachalam, K., Yang, X., & San, T. T. (2022). Tinospora cordifolia (Willd.) Miers: Protection mechanisms and strategies against oxidative stress-related diseases. J. Ethnopharmacol., 283, 114540.
10. Saha, S., & Ghosh, S. (2012). Tinospora cordifolia: One plant, many roles. Anc. Sci. Life., 31(4), 151-159.
11. Sangani, S. R., Dabhi, R. C., Kawad, M., Parmar, J., Arya, P. S., Chauhan, R. J., ... & Ameta, R. K. (2023). Buchwald coupling promoted benign synthesis of benzoxazine derivatives supported Cu complexes with their multipurpose potential in antimicrobial and catalytical fields. J. Mol. Struct., 1285, 135380.
12. Kawad, M., Sangani, S., Parmar, J., Dabhi, R. C., Arya, P. S., Teraiya, N., ... & Ameta, R. K. (2024). 2-Ferrocene-4-amine-1H-benzo [d] imidazole and their derivatives: Synthesis, biological and docking study. Polyhedron, 264, 117242.
13. Ashtekar, V., Dabhi, R. C., Trivedi, V. A., Arya, P. S., Patel, A., Thakor, P., ... & Patel, H. N. (2025). Functionalization of pyrazolo [1, 5-a] pyrazine-Schiff bases for assessing liquid crystalline properties and antimicrobial activity. J. Mol. Struct., 1335, 141889.